Lyophilization of NOTA-sdAbs

Baudhuin, Henri; Van Bockstal, Pieter-Jan; De Beer, Thomas; Vaneycken, Ilse; Bridoux, Jessica; Raes, Geert; Caveliers, Vicky; Keyaerts, Marleen; Devoogdt, Nick; Lahoutte, Tony; Xavier, Catarina

Published in:
European Journal of Pharmaceutics and Biopharmaceutics

DOI:
10.1016/j.ejpb.2021.06.012

Publication date:
2021

European Journal of Pharmaceutics and Biopharmaceutics 166 (2021) 194–204

Contents lists available at ScienceDirect

European Journal of Pharmaceutics and Biopharmaceutics

journal homepage: www.elsevier.com/locate/ejpb

Lyophilization of NOTA-sdAbs: First step towards a cold diagnostic kit for ^{68}Ga-labeling

Henri Baudhuin [a,*], Pieter-Jan Van Bockstal [b], Thomas De Beer [b], Ilse Vaneycken [a,e], Jessica Bridoux [a], Geert Raes [c,d], Vicky Caveliers [a,e], Marleen Keyaerts [a,e], Nick Devoogdt [a], Tony Lahoutte [a,e], Catarina Xavier [a]

[a] Department of Medical Imaging (MIMA), Vrije Universiteit Brussel, Brussels, Belgium
[b] Laboratory of Pharmaceutical Process Analytical Technology (LPPAT), Universiteit Gent, Ghent, Belgium
[c] Laboratory of Cellular and Molecular Immunology, Vrije Universiteit Brussel, Brussels, Belgium
[d] Myeloid Cell Immunology Laboratory, VIB Center for Inflammation Research, Brussels, Belgium
[e] Nuclear Medicine Department (NUCG), Universitair Ziekenhuis Brussel (UZ Brussel), Brussels, Belgium

ARTICLE INFO

Keywords:
Lyophilization
Radiopharmaceuticals
Cold kit
Gallium-68
PET imaging

ABSTRACT

Lyophilization is commonly used in the production of pharmaceutical compounds to increase the stability of the Active Pharmaceutical Ingredient (API) by removing solvents. This study investigates the possibility to lyophilize an anti-HER2 and an anti-MMR single-domain antibody fragment (sdAb)-based precursor as a first step in the development of a diagnostic kit for PET imaging.

Methods: NOTA-sdAb precursors have been lyophilized with the following formulation: 100 μg NOTA-sdAb in 0.1 M NaOAc (NaOAc), 5% (w/v%) mannitol-sucrose mix at a 2:1 ratio and 0.1 mg/mL polysorbate 80. During development of the formulation and drying cycle, factors such as cake appearance, glass transition temperature and residual moisture were analyzed to ensure qualitative and stable lyophilized samples. Stability studies of lyophilized precursor were conducted up to 18 months after storage at 2–8 °C by evaluating the precursor integrity, aggregation, functionality and ^{68}Ga-labeling efficiency. A comparative biodistribution study (lyophilized vs non-lyophilized precursor) was conducted in wild type mice (n = 3) and in tumor bearing mice (n = 6).

Results: The lyophilized NOTA-anti-HER2 precursor shows consistent stability data *in vitro* for up to 12 months at 2–8 °C in three separate batches, with results indicating stability even for up to T18m. No aggregation, degradation or activity loss was observed. Radiochemical purity after ^{68}Ga-labeling is consistent over a period of 12 months (RCP ≥ 95% at T12m). *In vivo* biodistribution analyses show a typical [^{68}Ga]Ga-NOTA-anti-HER2 sdAb distribution profile and a comparable tumor uptake for the lyophilized compound vs non-lyophilized (5.5% vs 5.7 %IA/g, respectively). *In vitro* results of lyophilized NOTA-anti-MMR precursor indicates stability for up to 18 months, while *in vivo* data show a comparable tumor uptake (2.5% vs 2.8 %IA/g, respectively) and no significant difference in kidney retention (49.4% vs 47.5 %IA/g, respectively).

Conclusion: A formulation and specific freeze-drying cycle were successfully developed to lyophilize NOTA-sdAb precursors for long-term storage at 2–8 °C. *In vivo* data show no negative impact of the lyophilization process on the *in vivo* behavior or functionality of the lyophilized precursor. These results highlight the potential to develop a kit for the preparation of ^{68}Ga-sdAb-based radiopharmaceuticals.

1. Introduction

Germanium-68/gallium-68 (^{68}Ge/^{68}Ga) generators are widely used in the preparation of ^{68}Ga-labeled radiotracers [1,2]. The introduction of these generators led to the development of new ^{68}Ga tracers [2–4] along with 'cold' kits [5–9], as it has been the case for [^{99m}Tc]Tc-based-tracers [10]. Such kits facilitate the distribution and storage of the precursor and allow a simple and standardized preparation of the

* Corresponding author at: ICMI, VUB, Laarbeeklaan 103, B-1090, Belgium.
E-mail addresses: Henri.Baudhuin@vub.be (H. Baudhuin), PieterJan.VanBockstal@UGent.be (P.-J. Van Bockstal), Thomas.DeBeer@UGent.be (T. De Beer), Ilse.Vaneycken@uzbrussel.be (I. Vaneycken), Jessica.Bridoux@vub.be (J. Bridoux), Geert.Raes@vub.be (G. Raes), Vicky.Caveliers@uzbrussel.be (V. Caveliers), Marleen.Keyaerts@vub.be (M. Keyaerts), Nick.Devoogdt@vub.be (N. Devoogdt), Tony.Lahoutte@uzbrussel.be (T. Lahoutte), Catarina.Xavier@vub.be (C. Xavier).

https://doi.org/10.1016/j.ejpb.2021.06.012
Received 30 March 2021; Received in revised form 27 May 2021; Accepted 22 June 2021
Available online 27 June 2021

radioactive compound, consistently ensuring a qualitative product upon each preparation. The kit concept is quite attractive, especially for ^{68}Ga-labeling, as the preparation and usage of such tracers is greatly simplified. Buffer is added to the precursor, followed by the ^{68}Ga eluate from the generator, yielding high radiochemical purity (RCP) in only a matter of minutes. Furthermore, the preparation can be performed on-site, and the resulting radiopharmaceutical does not require additional purification or sterile filtration. Examples of approved kits for ^{68}Ga-labeling are the NETSPOT® (manufactured by Advanced Accelerator Applications (AAA)) with FDA market approval, SOMAKIT TOC® (manufactured by AAA) with European market approval for somatostatin positive Neuroendocrine Tumor (NET) diagnosis and ILLUMET™ (manufactured by Telix Pharmaceuticals) for diagnosis of Prostate-Specific Membrane Antigen (PSMA)-expressing prostate cancers with FDA approval for Investigational New Drug (IND)-research studies.

These kits rely on peptides as targeting vehicles for the delivery of the radionuclide to a specific *in vivo* target of disease, however, other types of targeting vehicles could also benefit from such a kit concept. One particular vehicle of interest are single-domain antibody fragments (sdAb) which have shown to be excellent targeting vehicles as well and have been at the basis of several molecular imaging tracers [11–15]. SdAbs (trade marked as Nanobodies by Ablynx) are the recombinantly-produced variable fragments of Heavy-chain only antibodies (HcAb), a particular type of antibodies found in the blood of *camelidea* [16]. These HcAb lack light chains and their antigen binding site consists of only one variable domain (compared to two domains in the conventional antibody) [17,18]. It is this single, small, fully functional variable domain that can be isolated and used as targeting vehicle for a variety of applications due to its unique characteristics [19]. SdAbs are small (12 – 15 kDa), have short plasma half-lives, strong affinity (nanomolar to picomolar range), great specificity, high *in vivo* stability and favor renal body clearance, leading to relatively low biological half-lives (ranging between 1 h and several hours for humans), which are ideal properties for tracers [20–25].

Since sdAbs are derived from HcAbs, they can be generated to virtually any target. This provides the potential for a wide field of applications, which lead, along with their favorable characteristics and compatibility with versatile (radio)chemistry (e.g. fluorination, iodination, metal coordination chemistry, protein modification, fluorescence chemistry etc.), to the development of a variety of sdAb-based tracers for both imaging [24] (molecular characterization [11,26], diagnosis [12,27,28], image-guided surgery [29]) and targeted radionuclide therapy (TRNT) [15,30–32].

Clinical development of these sdAb-based tracers has already been initiated, with a first tracer, targeting HER2, being investigated in a theranostic setting (where the basis of the tracer serves for both diagnostic and therapeutic purpose) in HER2-positive breast cancer: it is being investigated as [^{68}Ga]Ga-NOTA-anti-HER2 VHH1 in academic clinical trials (VUB – UZ Brussel) for diagnosis *via* PET/CT imaging with a completed Phase I safety study (EudraCT 2012–001135-31) [24] and two ongoing Phase II studies (EudraCT 2016–002164-13 – NCT03924466; EudraCT 2015–002328-24 – NCT03331601), while the [^{131}I]I-SGMIB-anti-HER2 VHH1 variant is being investigated in a corporate clinical trial (Precirix NV) for a therapeutic approach with a completed Phase I safety study (EudraCT 2015–004840-21/ NCT02683083) [25]. A second tracer, targeting the Macrophage Mannose Receptor (MMR) or CD206, has entered an academic Phase I/II study (VUB – UZ Brussel) as [^{68}Ga]Ga-NOTA-anti-MMR-VHH2 for the detection of protumorigenic MMR-expressing Tumor Associated Macrophages (TAM) [33] (EudraCT 2017–001471-23), with additional potential imaging applications of atherosclerotic plaques [26,34,35] or rheumatoid arthritis [36]. A third sdAb-tracer has been developed targeting Vascular Adhesion Molecule 1 (VCAM-1) and is being prepared for clinical investigation as [^{99m}Tc]Tc-VCAM-1 for imaging of atherosclerotic lesions via SPECT/CT [37] (Centre Hospitalier Universitaire Grenoble Alpes).

As for other ^{68}Ga-tracers [5–9,38–43], developing a 'cold' kit for ^{68}Ga-labeling of sdAb-based tracers would be greatly beneficial, as a kit-form would allow us to perform envisaged multi-centric studies and, ultimately, to commercialize these products. Lyophilization, a method to remove solvents (typically water) from solutions, is commonly applied to increase the stability of the kit precursor, and for pharmaceuticals in general, otherwise unstable in solution. With the advantages of lyophilization [44], the growing market of biopharmaceuticals has shown an increased interest in employing such a method on products for medical use [45–47]. Due to the relatively low stability of sdAbs in solution, requiring storage at low temperature (- 20 °C) to obtain a reasonable shelf-life, lyophilization could also be applied to increase the stability. The success of lyophilization would be an important (and indispensable) achievement as a first step towards the development of a practical, easy-to-use and commercially viable kit.

In this study, the anti-HER2 and the anti-MMR sdAbs were conjugated with *p*-SCN-Bn-NOTA, a bifunctional chelator for ^{68}Ga-labeling, and the lyophilization of the NOTA-sdAb precursors was evaluated in the context of developing a 'cold' diagnostic kit. Stability studies at 2–8 °C and *in vivo* experiments were conducted to assess the stability over time and the influence of the drying process on the *in vivo* behavior of the lyophilized precursor.

2. Materials & methods

All commercially obtained chemicals were of analytical grade. The recombinant anti-HER2 '2Rs15d/VHH1′ and anti-MMR 'MMR3.49/VHH2′ sdAb-proteins were produced without terminal tags by the VIB Protein Service Facility in *Pichia pastoris* and were formulated in PBS during the final batch purification. *p*-SCN-Bn-NOTA was purchased from Macrocyclics (Macrocyclics, Inc., Plano, TX, USA). High purity water for trace analysis (TraceSELECT™, Riedel-de-Haën, Honeywell Research Chemicals, Seelze, Germany) was used for the preparation of radiolabeling buffer. ^{68}Ga was obtained from ^{68}Ge/^{68}Ga Galli Eo™ generators (IRE ELiT, Fleurus, Belgium).

The ^{68}Ge/^{68}Ga generators used in this project were typically 8 to 9 months upon retrieval, after serving in clinical routine, with activities ranging between 300 and 550 MBq. The generators have clinical expiry date of 12 months, however, they were used past their expiry date during this project.

2.1. Chromatographic analysis

Size exclusion chromatography (SEC) purification of NOTA-sdAb was conducted on an NGC Chromatography system (Bio-Rad Laboratories, USA) using a Superdex 30 preparatory grade (PG) HiLoad 16/600 column (GE Healthcare Bio-Sciences AB, Uppsala, Sweden) at a flow rate of 1 mL/min (injected mass > 6 mg) or a Superdex Peptide 10/300GL column (GE Healthcare Bio-Sciences AB, Uppsala, Sweden) at a flow rate of 0.5 mL/min (injected mass < 6 mg) with 0.1 M NaOAc pH 7 (NaOAc trihydrate, VWR Chemicals, Leuven, Belgium) as mobile phase. The latter was also used for quality control and follow up of NOTA-sdAbs stability.

Quality control (QC) of [^{68}Ga]Ga-NOTA-sdAbs was performed on a Hitachi Chromaster Chromatography system (VWR, Leuven, Belgium) using SEC on a Superdex Peptide 3.2/300 column (GE Healthcare Bio-Sciences AB, Uppsala, Sweden) at a flow rate of 0.15 mL/min with 0.02 M PBS/0.28 M NaCl pH 7.4 (PBS Tablets, Merck, Darmstadt, Germany) as mobile phase. QC was also assayed with binderless glass microfiber paper that was impregnated with silica gel (instant thin layer chromatography, iTLC-SG) (Agilent Technologies, Diegem, Belgium) with 0.1 M sodium citrate pH 5 (Citric acid, trisodium salt, dihydrate – Citric acid monohydrate, Acros Organics, part of Thermo Fisher Scientific, Geel, Belgium) as mobile phase.

Examples of each chromatographic profile are provided in Sup. Fig. S1 to S4.

2.2. Conjugation of p-SCN-Bn-NOTA to sdAb proteins

SdAb proteins (Anti-HER2: 3 – 13 mg, 0.24 – 1.03 μmol; Anti-MMR: 10 – 16 mg, 0.79 – 1.26 μmol) were buffer-exchanged to 0.05 M sodium carbonate/0.15 M NaCl buffer (Sodium carbonate anhydrous – Sodium hydrogen Carbonate – Sodium Chloride, VWR Chemicals, Leuven, Belgium), pH 8.7, using PD-10 size exclusion disposable columns (GE Healthcare, Buckinghamshire, UK). Protein solution (1.5 – 2 mg/mL) was added to a ten-fold (anti-HER2) or twenty-fold (anti-MMR) molar excess *p*-SCN-Bn-NOTA, pH adjusted to 8.5 – 8.7 with 0.2 M Na_2CO_3. After 2 h incubation at room temperature (RT), the pH of the reaction mixture is lowered to pH 7.4 by adding 1 M HCl (Suprapur, Merck, Darmstadt, Germany). The NOTA-sdAb protein solution was loaded on a SEC column. The collected fractions containing the monomeric NOTA-sdAb protein were pooled and the solution was passed through a 0.22 μm filter. The protein concentration is determined by UV absorption at 280 nm (NOTA-anti-HER2 sdAb: $\varepsilon = 49690\ M^{-1}.cm^{-1}$, MW = 13303 g/mol; NOTA-anti-MMR sdAb: $\varepsilon = 40660\ M^{-1}.cm^{-1}$, MW = 13128 g/mol).

2.3. Formulation of the kit

Before lyophilization, samples were prepared by mixing the NOTA-sdAb precursor with the compounds of the designed formulation. A stock solution was prepared for each formulation compound. For 500 mL of stock solution, 16.65 g of D-Mannitol (≥98%, Sigma-Aldrich, St. Louis, MO, USA) and 8.35 g Sucrose (≥99.5%, Sigma-Aldrich, St. Louis, MO, USA) were weighed and transferred to a 500 mL glass bottle (SCHOTT, Mainz, Germany) to which 450 mL of highly pure water was added. Finally, 50 mg of Polysorbate 80 (Merck, Darmstadt, Germany) was added to the mixture and water was further added to reach a final volume of 500 mL.

A one mL stock solution was transferred in a glass vial (SCHOTT, type 1 Plus Glass Vial, ISO Standard, TopLine, Adelphi Healthcare Packaging, Haywards Heath, UK), to which the NOTA-sdAb precursor (100 μg, 50 – 100 μl) was added. The stopper (Westar, FluroTec® Laminated Freeze Dry Stopper, Bromobutyl 4023/50 Grey, Adelphi Healthcare Packaging, Haywards Heath, UK) was placed and samples were transferred to the freeze-dryer (Telstar, LyoBeta).

2.4. Freeze-drying process

The freeze-drying cycle was initiated by freezing the samples down to −45 °C (-1 °C/min) and maintaining that temperature for 1 h to solidify the samples. The temperature was then gradually increased (+1 °C/min) to −20 °C to initiate the annealing step, inducing the crystallization of mannitol. The samples were then returned to −45 °C for solidification for 1 h. After that, vacuum (100 μbar) was applied in the chamber and the temperature was gradually increased (+1 °C/min) to −30 °C, which marks the start of the primary drying. The primary drying was carried out for 15 h, after which a slow gradual temperature increase was performed (0.2 °C/min) up to 30 °C to initiate the secondary drying. The secondary drying was carried out for 8 h to obtain the desired residual moisture (RM) level of<1.5%. At the end of drying process, the vials are closed under controlled nitrogen conditions.

2.5. Modulated digital scanning Calorimetry (MDSC)

The glass transition temperature of the lyophilized product was determined *via* Modulated Differential Scanning Calorimetry (MDSC) using a differential scanning calorimeter Q2000 (TA instruments, Zellik, Belgium). Tzero pans (TA instruments, Zellik, Belgium) were filled with approximately 5 mg of the lyophilized material. The MDSC cell was constantly purged with dry nitrogen at a flow rate of 50 mL/min. The sample was initially cooled down to 0 °C. This temperature was maintained for 5 min. Subsequently the temperature was linearly increased until 175 °C at a heating rate of 5 °C/min. The modulation amplitude and period were set at 0.531 °C and 40 s, respectively. The analysis was conducted in duplicate. The thermograms were analyzed with TA Instruments Universal Analysis 2000 version 4.7A (TA Instruments, Zellik, Belgium). An example of analysis is provided in Sup. Fig. S5

2.6. Karl-Fischer (KF) titration

The RM content of the lyophilized product was determined using Karl Fischer titration. The freeze-dried product was reconstituted with a known volume of dry methanol (Sigma-Aldrich, St. Louis, MO, USA) and left to equilibrate for roughly 15 min. With the help of a syringe, a known volume of this solution was volumetrically removed from the vial, injected in the titration vessel of the Mettler Toledo V30 volumetric Karl Fischer titrator (Schwerzenbach, Switzerland) and titrated with Hydranal® titration solvent (Sigma-Aldrich, S. Louis, MO, USA). Prior to the measurement of the residual water, the moisture content of the dry methanol was determined in triplicate and subtracted from the result. The RM content of the freeze-dried product was determined on two vials.

2.7. SDS-PAGE

SDS-PAGE was performed on NOVEX Wedgewell 16% 10-well gel (Thermo Fischer Scientific, Carlsbad, CA, USA), where 10 and 2 μg of NOTA-sdAb was loaded in both reducing and non-reducing conditions. The gel was run at 150 V for 80 min, after which a Coomassie Blue staining was performed for detection. Gels were visualized with the Amersham 680RGB Imager (GE Healthcare Bio-Sciences AB, Uppsala, Sweden) and analyzed via the GE ImageQuant TL 1D v 8.2.0 analysis software. An example of analysis is provided in Sup. Fig. S6.

2.8. Western Blot

Western Blot (WB) was performed with 5 μg of NOTA-sdAb in both reducing and non-reducing conditions. The blotting was performed on a nitrocellulose paper (Biorad) at 100 V for 60 min. The membrane was blocked in blocking buffer overnight in the fridge (1 g of powder milk in 50 mL PBS) (Nestlé, Nidal 2).

The membrane was rinsed and incubated with a monospecific polyclonal primary rabbit anti-2Rs15d or anti-MMR3.49 antibody (1 μg/mL) for 1 h, then washed and incubated with a secondary goat anti-rabbit-IRDye800CW (LI-COR, 926–32211) antibody (0.1 μg/mL) for 1 h.

Membranes were scanned using the Odyssey Imaging system (LI-COR, Lincoln, NE, USA) with Odyssey Application software V3.0.21 at 700 nm with intensity of 5.0 and at 800 nm with an intensity of 1.5, with a resolution of 84 μm. An example is provided in Sup. Fig. S7.

2.9. Surface plasmon resonance

Surface Plasmon Resonance (SPR) was performed on a Biacore T200 (GE Healthcare) system as described previously [12,14]. Briefly, a CM5 chip was coated with either recombinant HER2Fc or recombinant hMMR via 1-ethyl-3-(-3-dimethylaminopropyl)carbodiimide (EDC) and *N*-hydroxysuccinimide (NHS) chemistry. The affinity was determined by flowing different concentrations of precursor over the immobilized protein. The obtained curves were fitted with a 1:1 sdAb:antigen binding model to calculate the binding parameters. A reference sample containing anti-HER2-His_6 or anti-MMR-His_6 sdAb was added during each run.

2.10. Mass spectrometry

The number of conjugated NOTA-molecules to the sdAb was determined by ESI-Q-ToF-MS, which was performed by the GIGA Proteomics Facility of the University of Liège (Belgium). Briefly, samples are ultrafiltrated using Amicon ultra filter (Millipore) with a 3 kDa cut-off

membrane to remove salts and then re-diluted in a 30% ACN, 0.5% formic acid, 25 mM ammonium acetate solution. The analysis was performed on a Synapt G2 HDMS mass spectrometer (Waters) in positive ion mode.

2.11. Preparation of [^{68}Ga]Ga-NOTA-sdAbs

The ^{68}Ge/^{68}Ga generator was eluted at most 24 h prior to radiolabeling to minimize zinc contents.

The lyophilized precursor (NOTA-sdAb) sample was first reconstituted with 1.1 mL 1 M NaOAc pH 5 (NaOAc trihydrate, VWR Chemicals, Leuven 3001, Belgium – Acetic acid, ≥ 99.8%, puriss. p.a., Sigma-Aldrich, St. Louis 63103, MO, USA), after which the full ^{68}Ga eluate (1 – 1.1 mL) was added. The sample was incubated for 10 min at RT and then analyzed for radiochemical purity by iTLC and SEC (radio-SEC: [^{68}Ga]Ga-NOTA-sdAb t_R = 9.04 min, σ = 0.08 min; ^{68}Ga-citrate t_R = 13.25 min, σ = 0.08 min; radio-iTLC-SG: [^{68}Ga]Ga-NOTA-sdAb R_f = 0, ^{68}Ga-citrate R_f = 1).

Radiolabeling of the non-lyophilized precursor was performed in a similar way by diluting a NOTA-sdAb sample in 0.1 M NaOAc, with 1.1 mL 1 M NaOAc pH 5. Unless specified otherwise, the lyophilization excipients were dissolved in the corresponding amounts as the lyophilized samples prior to radiolabeling.

2.12. Cell culture

The human ovarian cancer cell line SKOV3 (HER2$^+$) was obtained from American Type Culture Collection (ATCC, Manassas, VA, USA) and the cells were cultured as described previously [30].

The murine lung adenocarcinoma cell line 3LL-R, a subclone of the LLC cell line [48], was cultured in RPMI-based medium containing Pen/Strep (1%), L-Glu (1%), non-essential amino acids (1%) and 10% FBS (Gibco, Life Technologies).

2.13. Biodistribution and tumor targeting study

The mice were housed at 22 °C in 50–60% humidity with a light/dark cycle of 12 h in filter cages. Food pellets and water were provided *ad libitum*. For animal handling and processing of data technicians and researchers were not blinded.

All procedures followed the guidelines of the Belgian Council for Laboratory Animal Science under license LA1230272 and were approved by the Ethical Committee for Animal Experiments of the Vrije Universiteit Brussel (NOTA-anti-HER2-sdAb: license 18–272-2; NOTA-anti-MMR-sdAb: license 19–272-1)

2.13.1. NOTA-anti-HER2-sdAb

For the biodistribution study, six weeks old, healthy, female C57Bl/6 Jax strain were used from Charles-Rivers. For the experiment, mice (n = 3 per group) were injected with 11.0 MBq, σ = 0.9 MBq of [^{68}Ga]Ga-NOTA-anti-HER2-sdAb (5 μg), prepared from either lyophilized or non-lyophilized precursor.

For the tumor targeting study, six weeks old, athymic, immune-deficient, female Crl:NU(NCr)-Foxn1nu mice were purchased from Charles-Rivers. The mice were inoculated subcutaneously in the intra-scapular region with 10^7 HER2-expressing SKOV-3 cells. Tumors were grown for two months until a volume of 250 – 350 mm^3 was reached. For the experiment, HER2$^+$ tumor bearing mice (n = 6 per group) were injected with 17.8 MBq, σ = 0.8 MBq of [^{68}Ga]Ga-NOTA-anti-HER2-sdAb (5 μg), prepared from either lyophilized or non-lyophilized precursor.

2.13.2. NOTA-anti-MMR-sdAb

For the biodistribution study, six weeks old, healthy, female C57Bl/6 Jax strain were purchased from Charles-Rivers. The mice were inoculated subcutaneously at the right flank with 5 x10^5 3LL-R cells. Tumors were grown for 13 days, reaching a tumor volume of 309.9 mm^3, σ = 170.0 mm^3.

For the experiment, 3LL-R tumor bearing mice were injected with 13.1 MBq, σ = 1.4 MBq of [^{68}Ga]Ga-NOTA-anti-MMR-sdAb (5 μg), prepared with either lyophilized precursor (n = 4) or non-lyophilized precursor (n = 5). Mice were randomized in two groups based on tumor size, measured the day before the experiment.

All mice were sacrificed 80 min post-injection (p.i.) for organ collection. The organs were weighed and measured for radioactivity in a gamma-counter (Cobra II, Packard). Tissue/organ uptake was calculated and expressed as a percentage injected activity per gram (%IA/g), corrected for decay. All procedures on living animals were performed while the animals were under anesthesia by isoflurane (ABBOTT, Ottignies-LLN Belgium) (5% induction in a box and 2.5% maintenance via a nose-cone). Mean results with standard deviations of *ex vivo* biodistribution data are available in Supplemental Table 1 to 3.

2.14. Statistical analysis

An unpaired student *t*-test was performed to compare the significance of uptakes in each organ between the lyophilized and non-lyophilized compounds. $P < 0.05$ was considered as significant.

N.D. abbreviation stands for 'Not determined'.

3. Results

3.1. Lyophilization formulation

The first step in the process of lyophilization is to design a suitable formulation of excipients. The designed formulation (Table 1) consists of a mix of sucrose and mannitol (5% w/w_{water}%, 1:2 ratio), where the sucrose acts as lyo- and cryoprotectant for the precursor and the mannitol acts as bulking agent to obtain a strong and elegant cake structure. A small amount of polysorbate 80 is present as well, which serves as surfactant to minimize vial wall interaction, reduce sheer stress and improve the recovery after reconstitution. The amount of 0.1 M NaOAc depends on NOTA-sdAb concentration.

3.2. Lyophilization cycle development

The freeze-drying cycle was designed starting from a base cycle (freezing, primary and secondary drying), from which eventually the final cycle was developed. The base cycle was conducted with conservative settings to assess the potential and feasibility of lyophilizing the NOTA-sdAb. The samples were frozen down to −45 °C for two hours. Subsequently, the pressure was lowered, and the shelf temperature was gradually increased to −30 °C, initiating primary drying. The primary drying time was set at 30 h and was followed by a second gradual temperature increase to 20 °C to initiate the secondary drying. The secondary drying was set at nine hours.

Due to a relatively low Tg of the dried samples using the base cycle (Tg ≈ 16 °C), we evaluated the possibility to add an annealing step. This annealing step is performed at the beginning of the drying process to induce crystallization of the mannitol. As such, a strong structure is created at the beginning of the process, which improved the drying

Table 1
Freeze-drying formulation.

Compound type	Specific compound	Amount
API	NOTA-sdAb in 0.1 M NaOAc	100 μg 50–100 μL
Lyo- and cryoprotectant	Sucrose	16.7 mg/mL
Bulking agent	Mannitol	33.3 mg/mL
Surfactant	Polysorbate 80	0.1 mg/mL

API = active pharmaceutical ingredient.

process and increased the stability of the dried samples (Tg ≈ 30 °C).

The base cycle was redesigned to incorporate the annealing step, to reduce the primary drying process, which had been monitored with in-process tools (comparative pressure measurement) [49], and finally to increase the secondary drying temperature in an attempt to further reduce the RM content and so increase the Tg of the dried samples (Tg ≈ 70 °C), resulting in the final freeze-drying cycle (Table 2).

3.3. Dried product

We set out to lyophilize the precursors in an all-in-one formulation. As such, we attempted to lyophilize the tracer in a formulation comprising the excipients (mannitol and sucrose) along with the NaOAc buffer required for the radiolabeling. By doing so, we hoped to obtain a true one-step labeling procedure, where the ^{68}Ga eluate could directly be added into the lyophilized vial for reconstitution and radiolabeling.

We tested different concentration of NaOAc (1 M, 0.6 M and 0.2 M); however, even for the lowest concentration, the lyophilization resulted in an unsatisfactory cake with a high RM content (>4%) and low long-term stability. Degradation of the precursor was observed within one month for the high concentration and within two months for the lowest, while stored at 2 – 8 °C.

Additional analysis of a 0.3 M NaOAc solution, containing 5% or 60% mannitol ($w_{mannitol}/w_{totalexcipients}$%), *via* MDSC to assess mannitol crystallization revealed that even with 60% mannitol no crystallization of this bulking agent occurred, which explains the collapsed cakes after freeze-drying of the previously lyophilized samples, as no crystal structure is present to provide support.

From these first experiments it became clear that an all-in-one formulation was unlikely to be successful. As such, we opted to separate the buffer from the formulation, resulting in a two-step preparation procedure: (i) reconstitution of the lyophilized precursor with 1 M NaOAc buffer pH 5 and (ii) addition of the ^{68}Ga eluate to the reconstituted precursor to start the labeling reaction.

From this point, the formulation and drying cycle were further developed, which included the addition of an annealing step, reduction of total processing time and temperature adaptations, leading to the final cycle described earlier. Although for each development and optimization step new batches were produced, only the stability data of final batches are presented here.

Upon lyophilization, the obtained dried product was inspected visually and provided a white elegant cake in the vial that can withstand firm shaking (example provided in Sup. Fig. S8).

To investigate the influence of variable amounts of NaOAc, which can vary depending on the NOTA-sdAb sample volume, on the dried product, different amounts of NaOAc were added to vials containing the formulation and the samples were lyophilized. The dried product was then analyzed for residual moisture content (RM) and glass transition temperature (Tg) in duplicate (Table 3). No difference in Tg and RM content was observed for amounts of 0.1 M NaOAc ranging from 0 to 150 µL.

Dried samples were placed in a fridge at 2 – 8 °C for stability studies and reconstitution of a sample was performed at the timepoint of stability testing with either 200 µl Milli-Q water for non-radioactive tests or with 1.1 mL of radiolabeling buffer for the radioactive tests.

When reconstituting a sample for labeling, the cake dissolved instantly upon addition of the radiolabeling buffer. After 10 s of gently swirling, no visible particles were present in the solution.

The non-radioactive tests (SDS-PAGE, WB, SEC, SPR, UV/VIS, KF titration, MDSC) were performed to assess the characteristics of the dried product, such as Tg and RM content, as well as the functionality and the potential aggregation of the precursor, while the radioactive tests (iTLC, SEC, pH) were performed to assess the labeling potential and to assess the integrity of the precursor.

The given specifications are requirements, which the future GMP product should meet and serve during this development phase as reference points to assess where further optimization is required.

3.4. Stability studies of the NOTA-anti-HER2 precursor

In a first batch, the NOTA-anti-HER2 precursor remained stable up to at least 18 months at 2 – 8 °C as no further aggregation could be observed (assessed *via* SEC and SDS-PAGE), the integrity as well as the radiolabeling potential was retained (assessed *via* radio-iTLC and radio-SEC after ^{68}Ga-labeling) and the functionality was preserved (assessed *via* SPR) (Tables 4 and 5). An increase in RM from 1.5% to 2.1% was observed from a freshly produced sample versus a sample stored at 2 – 8 °C for 18 months. This could well be within the measurement error; however, it is also likely that, over time, small amounts of moisture are attracted into the sample. The Tg decreased from 69 °C at T0 to 47 °C after 18 months. The increased RM over time is likely a contributing factor to the decreased Tg. The reduced RCP for T1m and T3m are most likely due to lower quality eluates, a potential combination of less frequent elution and the passing of the expiry date of the generator (for clinical use) (Table 5).

A second batch was monitored for 12 months (Tables 6 and 7) that remained stable for that period, supporting the stability data of the first batch. Surprisingly the measured Tg at T0 was considerably lower than the first batch (32 °C vs 69 °C). Although the RM also increased over time from 1.2% to 2.1%, the Tg increased from 32 °C to 43 °C at T0 and T12m, respectively. The low Tg at T0 could be attributed to moisture uptake during sample preparation, as the dried product is highly hygroscopic, and sample handling was not performed in a controlled environment. The reduced RCP for T6m is again most likely due to lower quality ^{68}Ga eluates.

A third batch was monitored for up to 18 months and confirms the stability data of the lyophilized NOTA-anti-HER2 samples (Tables 8 and

Table 2
Final freeze-drying cycle.

Process step	Shelf Temperature (°C)	Pressure (mbar)	Time (hh:mm)	Speed
Precooling shelves	3	-	-	-
Freezing	−45	-	00:48	−1 °C /min
Freezing	−45	-	1:00	-
Freezing (Annealing)	−20	-	0:25	1 °C/min
Freezing (Annealing)	−20	-	2:00	-
Freezing (Annealing)	−45	-	0:25	−1 °C /min
Freezing	−45	-	01:00	-
Chamber vacuum	−45	0.100	-	-
Primary drying	−30	0.100	00:17	1 °C/min
Primary drying	−30	0.100	15:00	-
Secondary drying	30	0.100	05:00	0.2 °C/ min
Secondary drying	30	0.100	08:00	-
Total time	-	-	33:55	-

Table 3
Influence of NaOAc on Tg and RM of dried product.

Volume of 0.1 M NaOAc	Tg (°C)	RM (%)
0 µL	61.1	0.95
25 µL	61.9	0.93
50 µL	59.6	0.61
75 µL	61.9	0.82
100 µL	60.8	0.90
150 µL	61.5	0.70

Table 4
Stability analyses of the NOTA-anti-HER2 Batch 1 – Non-radioactive tests.

Characterization test	Method	Specification	T0	T1m	T3m	T6m	T9m	T12m	T15m	T18m
Protein concentration (mg/mL)	UV absorbance	Report result	0.43	0.47	0.47	0.48	0.47	0.45	0.46	0.45
Profile by SDS-PAGE and CBB staining	SDS-PAGE	Major band between 10 and 15 kDa	OK	OK	OK	OK	OK	OK	OK	OK
Protein profile by gel filtration (%)	Analytical SEC	≥ 95%	99.2	99.1	99.1	99.0	99.3	99.4	99.5	99.4
Potency (nM)*	SPR	Report result	ND	3.6 Ref: 3.1	5.6 Ref: 3.1	ND	ND	6.3 Ref: 5.1	5.6 Ref: 3.7	7.4 Ref: 4.7
Residual Moisture (%)	KF-titration	Report result	1.5	-	-	-	-	-	-	2.1
Tg (°C)	MDSC	Report result	69	-	-	-	-	-	-	47

* Ref: anti-HER2-His_6.

Table 5
Stability analyses of the NOTA-anti-HER2 Batch 1 – Radioactive tests.

Characterization test	Method	Specification	T0	T1m	T3m	T6m*	T9m	T12m	T15m*	T18m
pH	pH meter	4 to 5	4.69	4.66	4.65	4.41	4.72	4.65	4.61	4.64
Radiochemical purity (%)	iTLC	≥ 95%	94	91	93	97	95	96	97	96
Radiochemical purity (%)	Analytical SEC	≥ 95%	95	93	95	ND	ND	97	98	97

* Depicts the timepoints when a recent ^{68}Ga generator was received from the hospital.

Table 6
Stability analysis of the NOTA-anti-HER2 Batch 2 – Non-radioactive tests.

Characterization test	Method	Specification	T0	T1m	T3m	T6m	T9m	T12m
Protein concentration (mg/mL)	UV absorbance	Report result	0.51	0.54	0.52	0.53	0.52	0.50
Profile by SDS-PAGE and CBB staining	SDS-PAGE	Major band between 10 and 15 kDa	OK	OK	OK	OK	OK	OK
Identification by Western Blot	Membrane blotting	Major band between 10 and 15 kDa ≥ 95%	OK	-	-	-	-	-
Protein profile by gel filtration (%)	Analytical SEC	≥ 95%	99.5	99.6	99.7	99.5	99.6	99.6
Potency (nM)*	SPR	Report result	3.8 Ref: 4.1	ND	4.1 Ref: 3.4	5.0 Ref: 5.1	ND	4.7 Ref: 4.7
Residual Moisture (%)	KF-titration	Report result	1.2	-	-	-	-	2.1
Tg (°C)	MDSC	Report result	32	-	-	-	-	43

* Ref: anti-HER2-His_6.

Table 7
Stability analysis of the NOTA-anti-HER2 Batch 2 – Radioactive tests.

Characterization test	Method	Specification	T0*	T1m	T3m	T6m	T9m*	T12m
pH	pH meter	4 to 5	4.55	4.62	4.65	4.57	4.64	4.67
Radiochemical purity (%)	iTLC	≥ 95%	99	97	96	91	98	93
Radiochemical purity (%)	Analytical SEC	≥ 95%	ND	ND	ND	93	99	97

* Depicts the timepoints when a recent ^{68}Ga generator was received from the hospital.

Table 8
Stability analysis of the NOTA-anti-HER2 Batch 3 – Non-radioactive tests.

Characterization test	Method	Specification	T0	T1m	T3m	T6m	T9m	T12m	T15m	T18m
Protein concentration (mg/mL)	UV absorbance	Report result	0.53	0.55	0.54	0.54	0.56	0.55	0.52	0.56
Profile by SDS-PAGE and CBB staining	SDS-PAGE	Major band between 10 and 15 kDa	OK	OK	OK	OK	OK	OK	OK	OK
Identification by Western Blot	Membrane blotting	Major band between 10 and 15 kDa ≥ 95%	OK	-	-	-	-	-	-	-
Protein profile by gel filtration (%)	Analytical SEC	≥ 95%	99.8	99.6	99.7	99.8	99.7	99.7	99.7	99.9
Potency (nM)*	SPR	Report result	4.4 Ref: 4.6	ND	4.2 Ref: 3.6	3.9 Ref: 3.2	4.4 Ref: 3.2	3.4 Ref: 3.2	ND	3.6 Ref: 2.7
Residual Moisture (%)	KF-titration	Report result	0.8	-	-	-	-	2.6	-	-
Tg (°C)	MDSC	Report result	49	-	-	-	-	40	-	-

* Ref: anti-HER2-His_6

Table 9
Stability analysis of the NOTA-anti-HER2 Batch 3 – Radioactive tests.

Characterization test	Method	Specification	T0	T1m	T3m*	T6m	T9m*	T12m	T15m	T18m
pH	pH meter	4 to 5	4.67	4.61	4.53	4.72	4.90	4.85	4.83	4.59
Radiochemical purity (%)	iTLC	≥ 95%	94	78	89	98	98	98	97	99
Radiochemical purity (%)	Analytical SEC	≥ 95%	98	94	92	98	ND	97	97	99

* Depicts the timepoints when a recent ^{68}Ga generator was received from the hospital.

9). A low RM content of 0.8% and Tg of 49 °C at T0 on this third batch already confirm the quality of the dried product. A high RCP was obtained even at T18m. In concordance with previous batches, after 12 months of storage an increase in RM from 0.8% to 2.6% occurred, while the Tg decreased from 49 °C to 40 °C. The reduced RCP at T1m was due to impurities, however, the strong difference in iTLC and SEC result is unclear. The lower RCP at T3m was probably due to radiolysis (degradation of the tracer by radioactivity-induced radicals), as that generator provided a relatively high activity of 620 MBq for the labeling at that timepoint. Radiolysis has clearly been observed during high activity radiolabelings (>850 MBq) and can be detected via iTLC and SEC with the observation of a peak with $R_f = 0.73$, $\sigma = 0.08$ (vs $R_f = 1.13$, $\sigma = 0.06$ for unlabeled ^{68}Ga (^{68}Ga-citrate)) and $R_t = 8.3$ min, $\sigma = 0.25$ min (vs $R_t = 7.6$ min, $\sigma = 0.34$ min for unlabeled ^{68}Ga (^{68}Ga-citrate)), respectively.

3.5. Stability studies of the NOTA-anti-MMR precursor

One batch of NOTA-anti-MMR precursor was lyophilized and monitored for up to 15 months (Tables 10 and 11) in parallel with NOTA-anti-HER2 Batch 1. The non-radioactive tests show consistent results for up to 15 months at 2 – 8 °C, with a high Tg (72 °C) and low RM content (1.7%) at T0. The results of the radioactive tests, however, are inconsistent over time (ranging between 70% – 96%). Switching to ultra-pure water for the preparation of the radiolabeling buffer from T6m on increased the RCP. However, inconsistent RCP was still observed at later timepoints, which could indicate instability of the precursor. Unfortunately, no samples were available for Tg and RM analysis at T15m.

A second batch of NOTA-anti-MMR was lyophilized and monitored for up to 18 months (Tables 12 and 13) in parallel with NOTA-anti-HER2 Batch 3. This second batch shows more consistent RCP over time with a high RCP even at T18m along with a Tg of 40 °C and RM content of 1.1% at T0. After 12 months of storage, the RM increased from 1.1% to 2.5%, while the Tg remained at 40 °C. It is likely that again moisture uptake during sample preparation influenced the Tg at T0, resulting in a lower temperature. This batch, however, indicates that the lyophilized NOTA-anti-MMR is stable for up to 18 months and suggests that the lower RCPs in the previous batch are more likely due to impurities in samples and lower quality eluates rather than instability. In the production of this second batch, high purity water was also used for the preparation of all necessary solutions necessary involved in the process.

3.6. In vivo studies

3.6.1. In vivo evaluation of [^{68}Ga]Ga-NOTA-anti-HER2

A direct comparison of the biodistribution in naive mice between the [^{68}Ga]Ga-NOTA-anti-HER2, produced *via* the lyophilized kit or not, was performed (Fig. 1). Only the kidneys show a significantly higher ($P < 0.05$) retention of the tracer ([^{68}Ga]Ga-NOTA-anti-HER2) prepared *via* the lyophilized precursor (43.44 %IA/g, $\sigma = 3.42\%$) versus the non-lyophilized precursor (33.55 %IA/g, $\sigma = 3.95\%$), while the lungs and liver show no significantly different uptake (lungs: 0.67 %IA/g, $\sigma = 0.25\%$ vs 0.61 %IA/g, $\sigma = 0.26\%$, with $P = 0.69$; liver: 1.43 %IA/g, $\sigma = 0.40\%$ vs 0.67 %IA/g, $\sigma = 0.26\%$ with $P = 0.053$; lyophilized vs non-lyophilized, respectively). Organs below 0.5% IA/g were considered as background uptake. Importantly, the lyophilization excipients were not added to the non-lyophilized tracer in this study.

A direct comparison on the functionality of the tracer, prepared from lyophilized or non-lyophilized precursor, was conducted in tumor bearing mice (Fig. 2). The tumor uptake shows no significant difference (5.45 %IA/g, $\sigma = 0.91\%$ vs 5.66 %IA/g, $\sigma = 2.48\%$ with $P = 0.85$), while kidneys show a significantly lower ($P < 0.001$) uptake for the lyophilized tracer (28.91 %IA/g, $\sigma = 3.59\%$) versus the non-lyophilized tracer (42.92 %IA/g, $\sigma = 4.98\%$). The lungs and liver did not show a significant different uptake (lungs: 0.49 %IA/g, $\sigma = 0.13\%$ vs 0.71 %IA/g, $\sigma = 0.26\%$, with $P = 0.09$; liver: 0.98 %IA/g, $\sigma = 0.21\%$ vs 1.16 %IA/g, $\sigma = 0.46\%$, with $P = 0.40$, lyophilized vs non-lyophilized, respectively). Organs below 0.5% IA/g were considered as background uptake.

3.6.2. In vivo evaluation of [^{68}Ga]Ga-NOTA-anti-MMR

In this study (Fig. 3), the tumor uptake shows no significant difference in uptake between the lyophilized ($n = 4$) and non-lyophilized ($n = 5$) NOTA-anti-MMR precursor (tumor: 2.49 %IA/g, $\sigma = 0.06\%$ vs 2.84 %IA/g, $\sigma = 0.52\%$, with $P = 0.31$, lyophilized vs non-lyophilized, respectively), while following organs did show a significantly different uptake: blood (0.71 %IA/g, $\sigma = 0.09$ vs 0.58, $\sigma = 0.05$, with $P < 0.05$), lungs (1.28%, $\sigma = 0.11\%$ vs 1.72, $\sigma = 0.17$, with $P < 0.01$), liver (5.47%, $\sigma = 0.32\%$ vs 6.29%, $\sigma = 0.35\%$, with $P < 0.01$), stomach (1.46%, $\sigma = 0.09$ vs 2.43%, $\sigma = 0.75$, with $P < 0.05$), muscle (0.57%, $\sigma = 0.08\%$ vs 0.79%, $\sigma = 0.09\%$, with $P < 0.01$), bone (1.25%, $\sigma = 0.18\%$ vs 1.58%, $\sigma = 0.17\%$, with $P < 0.05$, lyophilized vs non-lyophilized, respectively). MMR is known to have expression in different organs, therefore higher uptake values such as liver, spleen and lymph nodes was expected. Specificity of the [^{68}Ga]Ga-NOTA-anti-MMR tracer has previously been shown in MMR knock-out (KO) mice [33].

Table 10
Stability analysis of the NOTA-anti-MMR Batch 1 – Non-radioactive tests.

Characterization test	Method	Specification	T0	T1m	T3m	T6m	T9m	T11m	T12m	T15m
Protein concentration (mg/mL)	UV absorbance	Report result	0.50	0.48	0.47	0.46	0.48	0.49	0.46	0.48
Profile by SDS-PAGE and CBB staining	SDS-PAGE	Major band between 10 and 15 kDa	ND	OK	OK	OK	OK	OK	OK	OK
Protein profile by gelfiltration (%)	Analytical SEC	≥ 95%	99.6	99.6	99.4	99.5	99.6	99.6	99.6	99.6
Potency (nM)*	SPR	Report result	ND	ND	1.0 Ref: 0.7	ND	1.2 Ref: 1.2	ND	1.1 Ref: 1.1	ND
Residual Moisture (%)	KF-titration	Report result	1.7	-	-	-	-	-	-	-
Tg (°C)	MDSC	Report result	72	-	-	-	-	-	-	-

* Ref: anti-MMR3.49-His$_6$.

Table 11
Stability analysis of the NOTA-anti-MMR Batch 1 – Radioactive tests.

Characterization test	Method	Specification	T0	T1m	T3m	T6m*	T9m	T11m	T12m	T15m*
pH	pH meter	4 to 5	4.70	4.65	4.63	4.50	4.74	4.81	4.80	4.61
Radiochemical purity (%)	iTLC	≥ 95%	81	70	91	96	94	94	90	70
Radiochemical purity (%)	Analytical SEC	≥ 95%	90	93	93	ND	ND	96	95	83

* Depicts the timepoints when a recent ^{68}Ga generator was received from the hospital.

Table 12
Stability analysis of the NOTA-anti-MMR Batch 2 – Non-radioactive tests.

Characterization test	Method	Specification	T0	T1m	T3m	T6m	T9m	T12m	T15m	T18m
Protein concentration (mg/mL)	UV absorbance	Report result	0.45	0.46	0.41	0.39	0.43	0.41	0.41	0.46
Profile by SDS-PAGE and CBB staining	SDS-PAGE	Major band between 10 and 15 kDa	OK	OK	OK	OK	OK	OK	OK	OK
Identification by Western Blot	Membrane blotting	Major band between 10 and 15 kDa ≥ 95%	OK	-	-	-	-	-	-	-
Protein profile by gelfiltration (%)	Analytical SEC	≥ 95%	99.6	98.7	99.6	99.6	99.5	99.8	99.7	99.6
Potency (nM)*	SPR	Report result	1.0 Ref: 0.7	ND	1.5 Ref: 1.5	1.5 Ref: 1.4	1.3 Ref: 1.4	1.4 Ref: 1.4	1.3 Ref: 1.4	0.7 Ref: 1.3
Residual Moisture (%)	KF-titration	Report result	1.1	-	-	-	-	2.5	-	-
Tg (°C)	MDSC	Report result	40	-	-	-	-	40	-	-

* Ref: anti-MMR3.49His$_6$.

Table 13
Stability analysis NOTA-anti-MMR Batch 2 – Radioactive tests.

Characterization test	Method	Specification	T0	T1m	T3m*	T6m	T9m*	T12m	T15m	T18m
pH	pH meter	4 to 5	4.64	4.59	4.63	4.72	4.85	4.87	4.83	4.56
Radiochemical purity (%)	iTLC	≥ 95%	98	98	93	98	99	98	99	99
Radiochemical purity (%)	Analytical SEC	≥ 95%	99	99	97	98	ND	97	99	99

* Depicts the timepoints when a recent ^{68}Ga generator was received from the hospital.

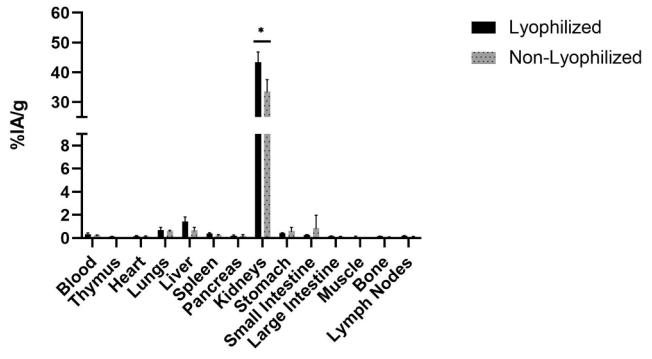

Fig. 1. Biodistribution profile of the [^{68}Ga]Ga-NOTA-anti-HER2 tracer prepared from the lyophilized or non-lyophilized precursor, in healthy C57Bl/6 mice (N = 3 per group). * P < 0.05.

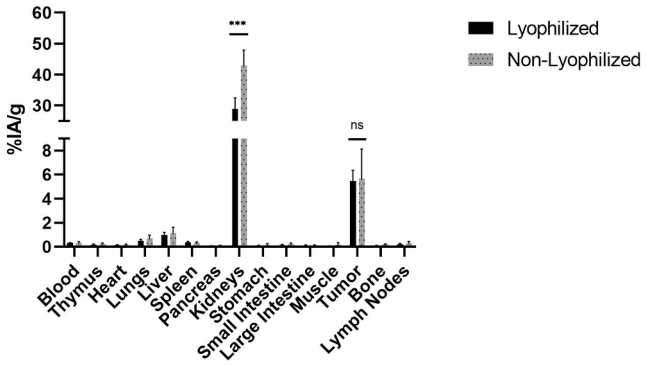

Fig. 2. Biodistribution profile of the [^{68}Ga]Ga-NOTA-anti-HER2 tracer prepared from the lyophilized or non-lyophilized precursor, in athymic tumor bearing NU-*Foxn1nu* mice (N = 6 per group). *** P < 0.001, ns = non-significance.

4. Discussion

To develop a kit for the preparation of ^{68}Ga-labeled sdAb tracers, we investigated the possibility to lyophilize the NOTA-sdAb precursor in order to increase the stability and facilitate their usage. Developing kits brings important advantages regarding the Chemistry, Manufacturing and Controls (CMC) and economical aspects, as they allow standardized and simplified preparation protocols and the ability for any center with a ^{68}Ge/^{68}Ga generator to prepare the radiopharmaceutical with minimal GMP license. As such, they allow multi-center studies in development phase and international distribution and commercialization upon market approval.

From the first lyophilization attempt, it became clear that adding high amounts of NaOAc to the formulation prevented crystallization of the bulking agent and led to an undesirable dried product. Therefore, the initial idea of an all-in-one formulation was reformed to a two-step 'reconstitution and labeling' procedure, like other ^{68}Ga kits, such as the SOMAKIT TOC® or the ILLUMET™ kit. To this date, to our knowledge, no real one-step labeling kit exists, due to the required buffer for the radiolabeling.

The resulting formulation, which provides protection of the precursor during and after lyophilization, is a simple but potent mix of sucrose and mannitol with a small amount of polysorbate 80, while the drying cycle provides an elegant cake and strong structure in the vial with

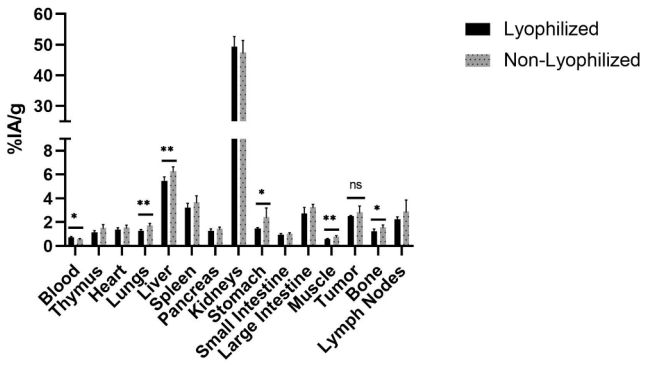

Fig. 3. Biodistribution profile of the [^{68}Ga]Ga-NOTA-anti-MMR tracer prepared from the lyophilized or non-lyophilized precursor, in tumor bearing C57Bl/6 mice (N = 4 and 5 per group, respectively). * $P < 0.05$, ** $P < 0.01$, ns = non-significance.

optimal features (high Tg and low RM content). The Tg remains high even after long periods of storage at 2 – 8 °C and, although variations in Tg between batches were measured, all measured Tg were still high (>30 °C) compared to the intended long-term storage temperature of 2 – 8 °C. Additionally, the presented freeze-drying cycle has been designed with conservative settings, allowing batch size upscaling with no or minimal alteration. For larger batches (>1000 vials), depending on the freeze-dryer capacity, we expect increasing the primary drying for up to 5 h the most likely (and only) alteration to be made.

The *in vitro* stability data of 3 batches shows that the lyophilized NOTA-anti-HER2 precursor is stable for at least 12 months, retaining full binding and labeling capacity, while stored at 2 – 8 °C. At 12 months of storage, no additional aggregation could be observed, while usually an RCP > 95% was achieved upon radiolabeling, indicating that the precursor is still intact. Additionally, the first batch and third batch show a stable behavior up to even 18 months of storage. Over time, an increase in residual moisture is observed, paired with a decrease in Tg. Moisture is likely attracted into the vial, due to the slight under pressure combined with the dryness of the inner vial. Moisture attraction in the vial can potentially be reduced by drying the stoppers before use and/or by reducing the under pressure in the final closed vial. The lower Tg, however, is still vastly above the storage temperature, and so the increased RM does not seem to compromise stability of the lyophilized product in our testing studies. Additionally, to avoid influence of moisture for the Tg analysis, sample preparation, handling and measurement should be performed in a low-humidity controlled environment

We observed important variances in RCP upon radiolabeling at different time points, which do not necessarily indicate instability of the product. Rather, we observed more variance after passing the clinical expiry date of the generator. It is important to note that with time the activity of ^{68}Ga eluate decreases, meaning that the ratio of impurity/activity can increase. This, in turn, can have important effects on the kinetics of the radiolabeling reaction, which would reduce the RCP. Typically, we observed an increase in RCP upon using a more recent generator. Additionally, the occurrence of radiolysis at higher activities warrants investigation of further adjustments to the formulation with potential radioprotectants (e.g. ascorbic acid).

In vivo data support the integrity and retention of functionality of the lyophilized precursor as a non-significant difference in tumor uptake in the tumor targeting study was obtained between the lyophilized and non-lyophilized tracer. A typical biodistribution profile for both conditions can be observed without main differences in profiles with exception of the kidneys. Excipients from the lyophilization formulation were thought to impact the kidney retention. For example, mannitol has been investigated as diuretic to reduce kidney retention of radiolabeled molecules, such as PSMA-targeting peptides, affibodies and DARPins, however, mannitol did not significantly alter kidney retention [50–52]. To rule out that the excipients from the herein developed formulation could influence the kidney retention, the same excipients were added to the tracer prepared from non-lyophilized precursor in the tumor targeting study. Overall, kidney retention in both studies were comparable or lower than previous results found during the development of the [^{68}Ga]Ga-NOTA-anti-HER2 tracer [27]. In general, influencing factors for kidney retention are natural mice variability and execution of the experiment at different timepoints during the day (e.g. morning vs afternoon).

The *in vitro* stability data of lyophilized NOTA-anti-MMR precursor shows a stability for up to at least 18 months. Although the first batch showed reduced RCP at 12 and 15 months, the non-radioactive tests of batch 1 suggest stability for up to 15 months, while stored at 2 – 8 °C. At 15 months of storage, no additional aggregation could be observed, however, the RCP dropped greatly (taking into account that radiolabelings were performed with buffers using high purity water from T6m and on), which suggested degradation of the precursor. The second batch shows more consistent RCP over time, indicating increased stability for up to 18 months, despite the reoccurring increase in RM. The favorable results of batch 2 imply that the reduced RCP of batch 1 at T12m and T15m could be attributed to impurities reducing the RCP and not degradation of the precursor. This second batch also showed the importance of using high purity compounds/starting materials (including the use of high purity water).

In vivo data of the [^{68}Ga]Ga-NOTA-anti-MMR tracer shows no significant difference in tumor uptake between the lyophilized and non-lyophilized precursor, which suggests that, as for the NOTA-anti-HER2, the lyophilized precursor retains its *in vivo* functionality. MMR is known to be expressed not only on macrophages but also on endothelial cells [53] and antigen-presenting cells [54] throughout the body, and on Kupffer cells in the liver [55], which results in uptake in organs such as liver, spleen, pancreas, lungs, lymph nodes and bone marrow. Previous imaging and biodistribution studies of [^{68}Ga]Ga-NOTA-anti-MMR and [^{18}F]FB-anti-MMR tracers have shown increased uptake in these organs, while specificity of the tracer was confirmed in MMR KO mice as the tracer uptake decreased to background or near background levels in all organs except kidneys [12,33]. The relatively low uptake values, along with small standard deviations, cause stringent conditions for the statistical *t*-test, which in turn results in a reported statistically significant difference in several organs.

The clearance of the [^{68}Ga]Ga-NOTA-anti-MMR tracer prepared from lyophilized or non-lyophilized precursor is similar as no significant difference in kidney retention was observed.

Overall the biodistribution of both [^{68}Ga]Ga-NOTA-anti-HER2 and [^{68}Ga]Ga-NOTA-anti-MMR tracers prepared from lyophilized precursors show a typical biodistribution profile, without major differences with their non-lyophilized counterpart, which indicate that the formulation and freeze-drying cycle is compatible for at least these two NOTA-sdAb precursors and that the designed formulation and drying cycle is a promising foundation for the further development of GMP-grade 'cold' diagnostic kits. Increase in RM over time is not expected to affect stability, as a relatively high Tg (well above storage temperature) is maintained.

Further development steps will comprise (1) adapting the mass of NOTA-sdAb per sample for radiolabeling with higher activity, to reduce inconsistent RCPs and to ensure a RCP > 95% upon each radiolabeling, (2) evaluating the addition of a radioprotectant to prevent radiolytic degradation of the tracers when using higher activities, (3) assessing the quality and choice of raw material based on purity, as it is imperative to use high purity products with low metal ion contents [56], and (4) evaluating the compatibility of the kit with ^{68}Ge/^{68}Ga generators from other manufacturers, such as E&Z and ITG. Additionally, the avenue of continuous freeze-dry manufacturing will be explored as well, as this can have important advantages compared to traditional batch freeze-drying [57]. Spin-freezing [58], a freezing technique that decreases layer

thickness and increases drying surface, which in turn vastly decreases primary drying time, as well as the use of dual chamber cartridges (DCC) (a type of cartridge, where the reconstitution solution is filled in a second chamber before the drying process, allowing quick and easy reconstitution after freeze-drying), in a continuous freeze-drying process [59], are both highly attractive factors that render the continuous drying process even more relevant and applicable for the kit production.

The work here presented could additionally directly benefit other NOTA-sdAb-based tracers, which are currently in development, such as the [^{68}Ga]Ga-NOTA-anti-CD20 tracer targeting CD20 for diagnosis in non-Hodgkin lymphoma [15] and the [^{68}Ga]Ga-NOTA-anti-PD-L1 tracer for PD-L1 immune checkpoint detection in developing tumors [60]. These tracers could be further developed in kit form as well before entering clinical translation.

Finally, although the work presented here was focused on creating a kit for ^{68}Ga-radiochemistry, the developed methods could potentially be applied to other sdAb-based precursors/tracers with other chelators, such as DTPA/DOTA-coupled sdAbs, for radiolabeling with other radionuclides, or to fluorescently labeled sdAbs, or even to other protein-/peptide based tracer, such as affibodies, as the advantages of increased stability and ease of distribution, coming from lyophilizing the precursor/tracer, might also apply. This could, in turn, widen the application of the methods described here and lead to kit development for such products as well.

5. Conclusion

The designed formulation and freeze-drying cycle allow us to further develop a kit for the preparation of the [^{68}Ga]Ga-NOTA-anti-HER2 and [^{68}Ga]Ga-NOTA-anti-MMR sdAbs. *In vivo*, we observe a non-significant difference in tumor uptake between the lyophilized and non-lyophilized compounds. This confirms that the lyophilized version of the [^{68}Ga]Ga-NOTA-sdAb tracer retains functionality after undergoing a stressful process. The next step is to optimize and finalize the complete kit product, followed by the preparations to produce the 'cold' kits under GMP conditions to obtain a clinical grade product, which would allow us to integrate the lyophilized precursors in ongoing clinical trials.

Financial support

This work has received support from the Industrial Research Fund (IOF), Scientific Fund W. Gepts UZ Brussel, IWT TBM (IWT.150198), Flemish League against Cancer, Foundation against Cancer and Fund for Scientific Research (FWO). M.K. and T.L. are senior clinical investigators of the Research Foundation-Flanders (FWO). J.B. is funded by the EU H2020 Marie Skłodowska-Curie Actions MSCA ITN PET3D N675417 and by the Scientific Fund W. Gepts UZ Brussel.

Funding sources solely provided financial support for the research.

Data availability statement

The raw data and processed data required to reproduce these findings are available to download from https://vub.sharepoint.com/:f:/r/teams/ORG-ICMI/External%20Share/Shared%20Documents/2021_Baudhuin%20et%20al_Lyo?csf = 1&web = 1&e = i3iUYH. Access can be granted upon request.

CRediT authorship contribution statement

Henri Baudhuin: Conceptualization, Methodology, Formal analysis, Writing - original draft, Visualization, Project administration. **Pieter-Jan Van Bockstal:** Conceptualization, Methodology, Formal analysis, Writing - original draft. **Thomas De Beer:** Conceptualization, Methodology, Validation, Resources. **Ilse Vaneycken:** Methodology, Writing - review & editing. **Jessica Bridoux:** Writing - review & editing. **Geert Raes:** Writing - review & editing. **Vicky Caveliers:** Writing - review & editing. **Marleen Keyaerts:** Writing - review & editing, Funding acquisition. **Nick Devoogdt:** Writing - review & editing. **Tony Lahoutte:** Validation, Resources, Supervision, Funding acquisition. **Catarina Xavier:** Methodology, Writing - review & editing, Visualization.

Declaration of Competing Interest

The authors would like to declare following potential competing interests: H.B. is co-founder of Abscint NV and has a first-line relative who is shareholder of Precirix NV. T.L. received honoraria from Precirix NV, Ion Beam Applications (IBA) and Institut des Radioéléments (IRE).T.L., N.D. and G.R. are co-founder of Abscint, co-founder of Precirix NV and consultant at Precirix NV. M.K. is co-founder of Abscint NV. M.K and V.C. received research funding from Precirix NV. T.L., N.D, G.R., M.K., V.C., C.X. and J.B. hold patents on sdAb imaging and therapy. Vrije Universiteit Brussel submitted patent applications comprising concepts depicted in this manuscript.

Acknowledgements

Phillipe Vanwolleghem provided valuable, constructive insights regarding practical development of (radio)pharmaceuticals, which helped in decision making and in shaping the outline of experiments.

GIGA Proteomics Facility of University of Liege, funded by FEDER and Waloon Region, for the generation of mass spectrometry data.

Special thanks to Cindy Peleman and Isabel Remory for their technical assistance during animal studies.

Appendix A. Supplementary data

Supplementary data to this article can be found online at https://doi.org/10.1016/j.ejpb.2021.06.012.

References

[1] I. Velikyan, 68Ga-Based radiopharmaceuticals: production and application relationship, Molecules 20 (2015) 12913–12943, https://doi.org/10.3390/molecules200712913.
[2] F. Rösch, Past, present and future of 68Ge/68Ga generators, Appl Radiat Isot 76 (2013) 24–30, https://doi.org/10.1016/j.apradiso.2012.10.012.
[3] I. Velikyan, Continued rapid growth in (68) Ga applications: update 2013 to June 2014, J Labelled Comp Radiopharm 58 (2015) 99–121, https://doi.org/10.1002/jlcr.3250.
[4] I. Velikyan, Prospective of 68 Ga Radionuclide Contribution to the Development of Imaging Agents for Infection and Inflammation, Contrast Media Mol Imaging 2018 (2018) 9713691, https://doi.org/10.1155/2018/9713691.
[5] T. Ebenhan, et al., Development of a Single Vial Kit Solution for Radiolabeling of 68Ga-DKFZ-PSMA-11 and Its Performance in Prostate Cancer Patients, Molecules 20 (2015) 14860–14878, https://doi.org/10.3390/molecules200814860.
[6] T. Ebenhan, et al., Evaluation of a Flexible NOTA-RGD Kit Solution Using Gallium-68 from Different, Mol Imaging Biol 19 (2017) 469–482, https://doi.org/10.1007/s11307-016-1014-1.
[7] A. Mukherjee, U. Pandey, R. Chakravarty, H.D. Sarma, A. Dash, Development of single vial kits for preparation of (68)Ga-labelled peptides for PET imaging of neuroendocrine tumours, Mol Imaging Biol 16 (2014) 550–557, https://doi.org/10.1007/s11307-014-0719-2.
[8] A. Amor-Coarasa, A. Milera, D. Carvajal, S. Gulec, A.J. McGoron, Lyophilized Kit for the Preparation of the PET Perfusion Agent [(68)Ga]-MAA, Int J Mol Imaging 2014 (2014), 269365, https://doi.org/10.1155/2014/269365.
[9] M.T. Ma, et al., Rapid kit-based 68Ga-labelling and PET imaging with THP-Tyr3-octreotate: a preliminary comparison with DOTA-Tyr3-octreotate, EJNMMI Research 5 (2015), https://doi.org/10.1186/s13550-015-0131-1.
[10] M.C.G. Valenzuela, et al., Technetium-99m Radiopharmaceuticals: Manufacture of Kits, Technical Reports Series 466 (2008).
[11] G. Bala, et al., Targeting of vascular cell adhesion molecule-1 by 18F-labelled nanobodies for PET/CT imaging of inflamed atherosclerotic plaques, Eur Heart J Cardiovasc Imaging 17 (2016) 1001–1008, https://doi.org/10.1093/ehjci/jev346.
[12] A. Blykers, et al., PET Imaging of Macrophage Mannose Receptor-Expressing Macrophages in Tumor Stroma Using 18F-Radiolabeled Camelid Single-Domain Antibody Fragments, J Nucl Med 56 (2015) 1265–1271, https://doi.org/10.2967/jnumed.115.156828.
[13] K. Broos, et al., Non-invasive assessment of murine PD-L1 levels in syngeneic tumor models by nuclear imaging with nanobody tracers, Oncotarget (2017), https://doi.org/10.18632/oncotarget.16708.
[14] I. Vaneycken, et al., Preclinical screening of anti-HER2 nanobodies for molecular imaging of breast cancer, FASEB J 25 (2011) 2433–2446, https://doi.org/10.1096/fj.10-180331.

[15] A. Krasniqi, et al., Theranostic Radiolabeled Anti-CD20 sdAb for Targeted Radionuclide Therapy of Non-Hodgkin Lymphoma, Mol Cancer Ther 16 (2017) 2828–2839, https://doi.org/10.1158/1535-7163.MCT-17-0554.
[16] D. Könning, et al., Camelid and shark single domain antibodies: structural features and therapeutic potential, Curr Opin Struct Biol 45 (2016) 10–16, https://doi.org/10.1016/j.sbi.2016.10.019.
[17] C. Hamers-Casterman, et al., Naturally occurring antibodies devoid of light chains, Nature 363 (1993) 446–448, https://doi.org/10.1038/363446a0.
[18] S. Muyldermans, T. Atarhouch, J. Saldanha, J.A. Barbosa, R. Hamers, Sequence and structure of VH domain from naturally occurring camel heavy chain immunoglobulins lacking light chains, Protein Eng 7 (1994) 1129–1135.
[19] G. Hassanzadeh-Ghassabeh, N. Devoogdt, P. De Pauw, C. Vincke, S. Muyldermans, Nanobodies and their potential applications, Nanomedicine (Lond) 8 (2013) 1013–1026, https://doi.org/10.2217/nnm.13.86.
[20] J. De Vos, N. Devoogdt, T. Lahoutte, S. Muyldermans, Camelid single-domain antibody-fragment engineering for (pre)clinical in vivo molecular imaging applications: adjusting the bullet to its target, Expert Opin Biol Ther 13 (2013) 1149–1160, https://doi.org/10.1517/14712598.2013.800478.
[21] P. Debie, N. Devoogdt, S. Hernot, Targeted Nanobody-Based Molecular Tracers for Nuclear Imaging and Image-Guided Surgery, Antibodies 8 (2019).
[22] Q. Lecocq, et al., Theranostics in immuno-oncology using nanobody derivatives, Theranostics 9 (2019) 7772–7791, https://doi.org/10.7150/thno.34941.
[23] A. Krasniqi, et al., Same-Day Imaging Using Small Proteins: Clinical Experience and Translational Prospects in Oncology, J Nucl Med 59 (2018) 885–891, https://doi.org/10.2967/jnumed.117.199901.
[24] M. Keyaerts, et al., Phase I Study of 68Ga-HER2-Nanobody for PET/CT Assessment of HER2 Expression in Breast Carcinoma, J Nucl Med 57 (2016) 27–33, https://doi.org/10.2967/jnumed.115.162024.
[25] M. D'Huyvetter, et al., Phase I trial of (131)I-GMIB-Anti-HER2-VHH1, a new promising candidate for HER2-targeted radionuclide therapy in breast cancer patients, J Nucl Med (2020), https://doi.org/10.2967/jnumed.120.255679.
[26] G. Bala, et al., Evaluation of [99m Tc]Radiolabeled Macrophage Mannose Receptor-Specific Nanobodies for Targeting of Atherosclerotic Lesions in Mice, Mol Imaging Biol 20 (2018) 260–267, https://doi.org/10.1007/s11307-017-1117-3.
[27] C. Xavier, et al., Synthesis, preclinical validation, dosimetry, and toxicity of 68Ga-NOTA-anti-HER2 Nanobodies for iPET imaging of HER2 receptor expression in cancer, J Nucl Med 54 (2013) 776–784, https://doi.org/10.2967/jnumed.112.111021.
[28] C. Xavier, et al., Clinical Translation of [68 Ga]Ga-NOTA-anti-MMR-sdAb for PET/CT Imaging of Protumorigenic Macrophages, Mol Imaging Biol (2019), https://doi.org/10.1007/s11307-018-01302-5.
[29] P. Debie, et al., Improved Debulking of Peritoneal Tumor Implants by Near-Infrared Fluorescent Nanobody Image Guidance in an Experimental Mouse Model, Mol Imaging Biol 20 (2018) 361–367, https://doi.org/10.1007/s11307-017-1134-2.
[30] M. D'Huyvetter, et al., Targeted radionuclide therapy with A 177Lu-labeled anti-HER2 nanobody, Theranostics 4 (2014) 708–720, https://doi.org/10.7150/thno.8156.
[31] M. D'Huyvetter, et al., I-labeled Anti-HER2 Camelid sdAb as a Theranostic Tool in Cancer Treatment, Clin Cancer Res 23 (2017) 6616–6628, https://doi.org/10.1158/1078-0432.CCR-17-0310.
[32] M. Pruszynski, M. D'Huyvetter, F. Bruchertseifer, A. Morgenstern, T. Lahoutte, Evaluation of an Anti-HER2 Nanobody Labeled with 225 Ac for Targeted α-Particle Therapy of Cancer, Mol Pharm 15 (2018) 1457–1466, https://doi.org/10.1021/acs.molpharmaceut.7b00985.
[33] C. Xavier, et al., Clinical Translation of 68Ga-NOTA-anti-MMR-sdAb for PET/CT Imaging of Protumorigenic Macrophages, Mol Imaging Biol (2019), https://doi.org/10.1007/s11307-018-01302-5.
[34] Z. Varasteh, et al., Targeting mannose receptor expression on macrophages in atherosclerotic plaques of apolipoprotein E-knockout mice using, EJNMMI Res 9 (2019) 5, https://doi.org/10.1186/s13550-019-0474-0.
[35] M.L. Senders, et al., Nanobody-Facilitated Multiparametric PET/MRI Phenotyping of Atherosclerosis, JACC Cardiovasc Imaging (2018), https://doi.org/10.1016/j.jcmg.2018.07.027.
[36] S. Put, et al., SPECT imaging of joint inflammation with Nanobodies targeting the macrophage mannose receptor in a mouse model for rheumatoid arthritis, J Nucl Med 54 (2013) 807–814, https://doi.org/10.2967/jnumed.112.111781.
[37] A. Broisat, et al., Nanobodies targeting mouse/human VCAM1 for the nuclear imaging of atherosclerotic lesions, Circ Res 110 (2012) 927–937, https://doi.org/10.1161/CIRCRESAHA.112.265140.
[38] D. Prince, D. Rossouw, S. Rubow, Optimization of a Labeling and Kit Preparation Method for Ga-68 Labeled DOTATATE, Using Cation Exchange Resin Purified Ga-68 Eluates Obtained from a Tin Dioxide, Mol Imaging Biol 20 (2018) 1008–1014, https://doi.org/10.1007/s11307-018-1195-x.
[39] J.D. Young, et al., Ga-THP-PSMA: A PET Imaging Agent for Prostate Cancer Offering Rapid, Room-Temperature, 1-Step Kit-Based Radiolabeling, J Nucl Med 58 (2017) 1270–1277, https://doi.org/10.2967/jnumed.117.191882.
[40] H.M. Yu, et al., Development of single vial kits for preparation of, J Labelled Comp Radiopharm 61 (2018) 885–894, https://doi.org/10.1002/jlcr.3673.
[41] A. Mukherjee, et al., Ga-NOTA-ubiquicidin fragment for PET imaging of infection: From bench to bedside, J Pharm Biomed Anal 159 (2018) 245–251, https://doi.org/10.1016/j.jpba.2018.06.064.
[42] B.Y. Yang, et al., Formulation of 68Ga BAPEN kit for myocardial positron emission tomography imaging and biodistribution study, Nucl Med Biol 37 (2010) 149–155, https://doi.org/10.1016/j.nucmedbio.2009.10.010.
[43] J. Seemann, B. Waldron, D. Parker, F. Roesch, DATATOC: a novel conjugate for kit-type, EJNMMI Radiopharm Chem 1 (2017) 4, https://doi.org/10.1186/s41181-016-0007-3.
[44] J.F. Carpenter, B.S. Chang, W. Garzon-Rodriguez, T.W. Randolph, Rational design of stable lyophilized protein formulations: theory and practice, Pharm Biotechnol 13 (2002) 109–133.
[45] W. Wang, S. Singh, D.L. Zeng, K. King, S. Nema, Antibody structure, instability, and formulation, J Pharm Sci 96 (2007) 1–26, https://doi.org/10.1002/jps.20727.
[46] W. Wang, Lyophilization and development of solid protein pharmaceuticals, Int J Pharm 203 (2000) 1–60.
[47] B.S. Chang, S. Hershenson, Practical approaches to protein formulation development, Pharm Biotechnol 13 (2002) 1–25.
[48] L.M. Remels, P.C. De Baetselier, Characterization of 3LL-tumor variants generated by in vitro macrophage-mediated selection, Int J Cancer 39 (1987) 343–352.
[49] S.M. Patel, M. Pikal, Process analytical technologies (PAT) in freeze-drying of parenteral products, Pharm Dev Technol 14 (2009) 567–587, https://doi.org/10.3109/10837450903295116.
[50] E.A.M. Ruigrok, W.M. van Weerden, J. Nonnekens, M. de Jong, The Future of PSMA-Targeted Radionuclide Therapy: An Overview of Recent Preclinical Research, Pharmaceutics 11 (2019), https://doi.org/10.3390/pharmaceutics11110560.
[51] M. Altai, H. Liu, A. Orlova, V. Tolmachev, T. Gräslund, Influence of molecular design on biodistribution and targeting properties of an Affibody-fused HER2-recognising anticancer toxin, Int J Oncol 49 (2016) 1185–1194, https://doi.org/10.3892/ijo.2016.3614.
[52] M. Altai, et al., On the prevention of kidney uptake of radiolabeled DARPins, EJNMMI Res 10 (2020) 7, https://doi.org/10.1186/s13550-020-0599-1.
[53] S.A. Linehan, L. Martínez-Pomares, P.D. Stahl, S. Gordon, Mannose receptor and its putative ligands in normal murine lymphoid and nonlymphoid organs: In situ expression of mannose receptor by selected macrophages, endothelial cells, perivascular microglia, and mesangial cells, but not dendritic cells, J Exp Med 189 (1999) 1961–1972, https://doi.org/10.1084/jem.189.12.1961.
[54] S.A. Linehan, The mannose receptor is expressed by subsets of APC in non-lymphoid organs, BMC Immunol 6 (2005) 4, https://doi.org/10.1186/1471-2172-6-4.
[55] M.E. Taylor, Structure and function of the macrophage mannose receptor, Results Probl Cell Differ 33 (2001) 105–121.
[56] R. Chakravarty, S. Chakraborty, A. Dash, M.R. Pillai, Detailed evaluation on the effect of metal ion impurities on complexation of generator eluted 68Ga with different bifunctional chelators, Nucl Med Biol 40 (2013) 197–205, https://doi.org/10.1016/j.nucmedbio.2012.11.001.
[57] P.J. Van Bockstal, L. De Meyer, J. Corver, C. Vervaet, T. De Beer, Noncontact Infrared-Mediated Heat Transfer During Continuous Freeze-Drying of Unit Doses, J Pharm Sci 106 (2017) 71–82, https://doi.org/10.1016/j.xphs.2016.05.003.
[58] P.J. Van Bockstal, et al., Mechanistic modelling of infrared mediated energy transfer during the primary drying step of a continuous freeze-drying process, Eur J Pharm Biopharm 114 (2017) 11–21, https://doi.org/10.1016/j.ejpb.2017.01.001.
[59] L. De Meyer, et al., Dual chamber cartridges in a continuous pharmaceutical freeze-drying concept: Determination of the optimal dynamic infrared heater temperature during primary drying, Int J Pharm 570 (2019), 118631, https://doi.org/10.1016/j.ijpharm.2019.118631.
[60] J. Bridoux, et al., Anti-human PD-L1 Nanobody for Immuno-PET Imaging: Validation of a Conjugation Strategy for Clinical Translation, Biomolecules 10 (2020), https://doi.org/10.3390/biom10101388.